Ellipsoid Zone Thickness in Sporadic Adult-Onset Foveomacular Vitelliform Dystrophy

Shayan Yousefi
Hadassah Medical Center   https://orcid.org/0000-0002-8968-4001

Liran Tiosano (✉ tiosanoliran@gmail.com)
Hadassah Medical Center

Tareq Jaouni
Hadassah Medical Center

Edward Averbukh
Hadassah Medical Center

Eyal Banin
Hadassah Medical Center

Tali Bdolah-Abram
Hebrew University Hadassah Medical School: The Hebrew University of Jerusalem School of Medicine

Itay Chowers
Hadassah Medical Center

Abstract

Purpose: To evaluate the thickness of the ellipsoid zone (EZ) layer and its correlation with visual acuity and the disease stage in eyes with Adult-onset foveomacular vitelliform dystrophy (AFVD).

Materials and Methods: Ninety-two eyes of 57 patients with AFVD were evaluated. Four consecutive spectral-domain optical coherence tomography (SD-OCT) scans from each study eye were analyzed. Retinal layers were segmented, and the EZ layer thickness was measure in two areas of the macula: at the center of fovea (CF) and at the foveal avascular zone edge (FE).

Results: The mean±SD EZ thickness for was 16.5±9.6 microns at the center of fovea (CF) and 17± 9.8 microns at the edge of foveal avascular zone (FE; p=0.006, t-test). Compared to 30 healthy eyes, the EZ was thicker at the vitelliform stage in both CF and FE (p<0.001 in both points, t-test), and during the pseudohypopyon or vitelliruptive stages in CF (p=0.007, t test), but not in edge of the fovea (p=0.15, t test). Visual acuity was better in eyes with intact EZ compared to absent EZ (p=0.001 for both CF and FE, ANOVA test). There was a trend for an association between EZ thickness and the stage of AFVD (p=0.06, ANOVA test).

Conclusion: The foveal EZ thickness in AFVD, is thicker comparing with controls. This might suggest that impaired retinal pigment epithelium phagocytosis or excess photoreceptor EZ production play important role in the pathogenesis of AFVD.

Background

Adult-onset foveomacular vitelliform dystrophy (AFVD) is a form of pattern dystrophy, which is characterized by bilateral, subretinal, symmetrical, yellowish round lesions in the macular region. AFVD typically appears in the fourth to sixth decades of life [1–2]. While monogenic etiology is associated with some cases of AFVD (e.g. PRPH2 or BEST1 gene mutations) [3–10] most of the AFVD patients do not carry mutations in these genes. Sporadic AFVD is the more common form of the disease, where patients lack mutations in genes which were previously associated with the phenotype. Such sporadic cases tend to present at a later age compared with monogenic AFVD, but, otherwise show a similar phenotype [11].

Extracellular photoreceptor debris and retinal pigment epithelium (RPE)-derived material, are deposited in the subretinal space to compose the vitelliform lesion in AFVD [12]. Vitelliform lesions are dynamic, showing lesion growth with accumulation of lipofuscin, following by partial or complete absorption of the material, disruption of the overlying photoreceptors and atrophy of the underlying RPE [13]. Impaired phagocytosis of shaded photoreceptor outer segment discs due to excess photoreceptor outer segment production, physical separation of the RPE from the photoreceptor, or RPE malfunction were suggested as underlying mechanisms for generation of the vitelliform lesions [1]. It is unclear which of these mechanisms or their combination is crucial for generation of the vitelliform lesions in AFVD.

The ellipsoid zone (EZ) as detected via spectral-domain optical coherence tomography (SD-OCT) imaging represents the ellipsoid component of the photoreceptors which are packed with mitochondria; identification of the EZ has critical prognostic value in macular disorders [14–15].

Intact EZ has been demonstrated to correlate with preserved visual acuity, while absent or disrupted EZ were correlated with altered visual acuity in AFVD [11,13,16–17]. Integrity and intensity of the EZ has been also shown to be reduced in several retinal degenerative conditions, inflammatory diseases, and in moderate and severe glaucoma [18–31].

While the EZ is readily identified in SD-OCT, segmentation and quantification of this layer may provide important insights into the AFVD [32–35]. To that end, we measured the thickness of the EZ and correlated it to clinical features in AFVD.

Methods

Patient demographics, clinical and imaging data were retrospectively collected on a consecutive group of AFVD cases. All patients were treated and followed in the retina service of the Department of Ophthalmology at the Hadassah-Hebrew University Medical Center in Jerusalem, Israel, between January 2010 and January 2017. Patients signed an informed consent form and the study was approved by the institutional ethics committee.

The EZ was segmented and evaluated using OCT (Spectralis - Heidelberg Engineering, Germany) scans from 92 eyes (n = 57 patients) with AFVD, which were included in a previous report on the long term follow up of the disease [11]. Inclusion and exclusion criteria for this cohort were previously described [11]. Briefly, patients with AFVD in at least one eye at any stage were included in the study. Vitelliform lesions associated with any other pathology, such as Best's disease, vitreomacular traction (VMT) or epiretinal membrane were excluded. Scans with poor image quality which hinder proper segmentation (shadow artifact, motion artifact, and noise) were excluded.

Four consecutive OCT scans from each study eye with an interval of 3 to 6 months between the visits were analyzed. For automated multi-layer retinal segmentation we used the 6.3a software version of the Spectralis SD-OCT. Based on the reflectivity of the different retinal layers, the software produced 13 lines representing the boundaries of the retinal layers: internal limiting membrane (ILM), retinal nerve fiber layer (RNFL), ganglion cell layer (GCL), inner plexiform layer (IPL), inner nuclear layer (INL), outer plexiform layer (OPL), outer nuclear layer (ONL), external limiting membrane (ELM), first photoreceptor layer (PR1), second photoreceptor layer (PR2), retinal pigment epithelium (RPE), bruch's membrane (BM), and choroid (CHO). However, the software does not measure the EZ. Based on the segmentation generated by the software we identified the EZ and measured its thickness (Fig. 1). To that end, we manually adjusted the lines that represent the RPE to the inner edge of the hypo-reflective area (zone 12) [14], and the outer retinal layer line to the hypo-reflective line of the myoid zone of the photoreceptors (Fig. 1). Finally, we subtracted the RPE layer thickness from the thickness of the outer retinal layer per the automatic measurement of the Spectralis software and got the thickness of the isolated ellipsoid zone layer. We

measured the thickness in two areas of the macula: at the center of fovea (CF), and at the edge of the foveal avascular zone (FAZ) 500 microns nasal to the fovea (FE) (Fig. 1). The nasal edge of retina is the thickest part so its measurement minimalizes measurement errors [36–37].

In addition to segmentation of the retina layers, the following features were also analyzed for each visit: (1) stage of the vitelliform lesion (vitelliform, vitelliruptive, pseudohypopyon and atrophy); (2) integrity of the EZ which was graded as intact, disrupted or absent; (3) presence of sub or intra retinal fluid (SRF, IRF), retinal pigment epithelial detachment (PED) or drusen (4) vitreoretinal interface abnormalities including ERM, VMT and posterior vitreous detachment (PVD).

The entire procedure was performed by two experiences graders (S.Y. and L.T.) in order to investigate the repeatability of all measurements. All values were then averaged to perform the statistical analysis.

Statistical analyses were performed using SPSS (version 25.0; IBM Corp., Armonk, NY). In order to evaluate a single OCT scan as a separate case, we used a repeated measures ANOVA model to evaluate the association of the change over time in the visual acuity with the progression of the stages. Comparing stage between different time points was performed using the McNemar-Bowker's test. To compare quantitative variables (e.g. months of follow-up) between two independent groups (change in stage, etc.) the Mann-Whitney non-parametric test was applied. The ANOVA test with post hoc comparisons with the Dunnett correction was used for comparing quantitative variables between three independent groups (e.g. visual acuity by thickness in fovea or in distance from fovea, in three categories). The Chi-square and the Fisher's exact tests were used for evaluating the association between two categorical variables (stage, etc.), and the linear by linear association test was used for assessing trend. Finally, Intraclass correlation coefficients (ICC) between graders was calculated for the EZ thickness and integrity. All tests applied were two-tailed and a p-value of 5% or less was considered statistically significant.

Results

Patients and Lesions Characteristics

A total of 92 eyes of 57 patients with AFVD were included in the study. The male/female ratio was 32/25 with a mean age (± SD) of 79.1 ± 11.7 years (range 30–98 years). Mean (± SD) follow up period was 14.9 ± 8.2 months (range 2–43 months, median 13 months). The patients had a mean ± SD of 3.07 ± 0.2 visits during the follow up. Thirty-five patients had bilateral lesion and 22 patients had unilateral. At baseline 22 eyes were at the vitelliform stage, 6 eyes were at the pseudohypopyon stage, 58 eyes were at the vitelliruptive stage and 6 eyes were at the atrophic stage.

Thirteen eyes (59%) in the vitelliform stage remained at the vitelliform stage during the entire follow up, nine (41%) of them progressed to the pseudohypopyon or vitelliruptive stage, and none of the eyes progressed to the atrophic stage. Sixty-two (97%) of eyes in pseudohypopyon or vitelliruptive stage

remained at the same stage during the entire follow up and two (3%) of them progressed to the atrophic stage.

The mean baseline and last visit visual acuity (± SD) of the entire cohort was 0.29 ± 0.22 LogMAR, and 0.30 ± 0.23 LogMAR, respectively (p = 0.732, paired t test). The vision remained stable during the entire study and there was no association or interaction between change in stage and follow-up time (p = 0.205, and p = 0.251, respectively, ANOVA test). As the model showed no association or interaction between stage, vision and time, we could regard each visit as a separated case to evaluate the association between visual acuity, stage and thickness of the EZ layer. Intraclass correlation coefficients between two graders for the central fovea EZ thickness was 0.921(95% confidence interval (CI) 0.884–0.931), for the edge of the fovea EZ thickness was 0.907(CI 0.874–0.927), and EZ integrity 0.911 (CI 0.866–0.937).

EZ thickness

A total of 282 individual OCT scans were collected and analyzed. The mean ± SD EZ thickness for the entire cohort was 16.54 ± 9.62 microns at the center of the fovea (CF) and 17.96 ± 9.76 microns at 500 microns nasal to the fovea (FE). The Mean EZ was thicker nasal to the fovea compared with the fovea (p = 0.006, t-test). Measurements of the foveal EZ thickness demonstrated 118 (42%) sections with EZ thicker than 20 microns, 108 (38%) sections with EZ thinner than 20 microns, and 56 (20%) sections where the EZ layer could not be detected. The reason we chose the number 20 microns as the cutoff between groups of EZ thickness is the fact that there is unclear information about EZ thickness in normal eyes. Itoh et al. reported a mean EZ thickness of 22 microns in unaffected eyes [35] but our normal control eyes had EZ thickness of 14.87 microns in fovea, so 20 microns is a reasonable cutoff.

The mean ± SD visual acuity of eyes with those sections was 0.23 ± 0.19, 0.25 ± 0.17, and 0.53 ± 0.26 LogMAR, respectively There was no difference in the visual acuity between sections with foveal EZ thickness > 20 microns to ones with EZ thickness < 20 microns (p = 0.28, ANOVA test); While visual acuity was better in eyes with EZ thickness < 20 microns and eyes where EZ was not identified (p = 0.001, ANOVA test; Fig. 2).

Measurement of the EZ thickness 500 microns nasal to the fovea center was performed to assess the correlation of EZ thickness in both points. At FE there were 130 (46%) sections with EZ thickness > 20 microns, 104 (37%) sections had EZ < 20 microns, and 48 (17%) sections without an identifiable EZ area. The mean ± SD visual acuity in these groups was 0.26 ± 0.19, 0.23 ± 0.16, and 0.54 ± 0.28 LogMAR, respectively. Eyes with am EZ > 20 microns had similar acuity compared with eyes with EZ < 20 microns (p = 0.31, ANOVA test), while eyes with EZ < 20 microns had better acuity compared with eyes without EZ (p = 0.001; ANOVA test; Fig. 2).

EZ thickness at the different stages of AFVD

Forty-five scans showed the vitelliform stage and the mean ± SD thickness at CF and FE was 19.49 ± 4.62 microns, and 20.44 ± 3.60, respectively (p = 0.192, t test). Two hundred and ten scans showed vitelliruptive or the pseudohypopyon stages and the mean ± SD thickness in CF was and FE was 17.14 ±

9.53 microns, and 18.27 ± 10.08 microns, respectively (p = 0.069, t test), while 27 scans showed an atrophic stage and the mean ± SD thickness in CF and FE was 6.89 ± 11.00 microns, and 11.37 ± 11.53 microns respectively (p = 0.028, t test). There was a trend for an association between EZ thickness and the stage of the vitelliform lesion (p = 0.06, ANOVA test).

We also measured the EZ thickness in normal control group that was composed of 30 healthy eyes (n = 16 patients) with mean age of 70 ± 5.82 years. The mean visual acuity of the 30 eyes was 0.0 LogMAR. The mean EZ thickness at CF and FE was 14.87 ± 2.82 microns, and 17.17 ± 1.84 microns, respectively. By comparison, the mean ± SD EZ thickness for the entire AFVD cohort at CF and FE was 16.54 ± 9.62 microns (p = 0.032 vs. controls, t test), and 17.96 ± 9.76 microns (p = 0.24 vs. controls, t test), respectively. We also compared the EZ thickness between normal control group and each stage separately. This analysis demonstrated thicker EZ at CF and FE of sections with vitelliform lesions (p < 0.001 in both points, t test). There was also thicker EZ in CF in sections with vitelliruptive or pseudohypopyon lesions compared with unaffected controls (p = 0.007, t test) but not in FE (p = 0.15, t test).

Discussion

In this retrospective study, we analyzed the thickness of the EZ in the fovea and at the edge of the FAZ in eyes affected by AFVD that do not carry mutations in genes that were previously associated with the phenotype. The clinical characteristics, visual acuity, and long-term follow up of these patients were previously reported [11].

The mean EZ thickness at the center of the fovea for the entire AFVD group in this study was approximately 17 micron while the normal controls had a thinner mean EZ in the fovea center of approximately 15 micron. By contrast, thicker EZ nasal to the fovea was detected in AFVD eyes only during the vitelliform stage but not during the vitelliruptive or pseudohypopyon stages compared with controls. Analysis of the data also demonstrated a trend towards thickened EZ in eyes at the vitelliform stage compared with ones at the vitelliruptive, psudohypopyn or atrophic stages.

Few data is available in the literature on EZ thickness. Itoh and colleagues reported a mean EZ thickness of 22 microns in 12 unaffected eyes, while eyes with geographic atrophy, mild hydroxychloroquine toxicity, and ocriplasmin treated eyes, had thinner EZ [35]. We and others have previously reported that the visual acuity of patients with AFVD correlates with the integrity and intensity of the EZ [11,13].

Excess EZ thickness may be associated with the pathogenesis of AFVD via few mechanisms. (1) Vitelliform lesions in AFVD may form due to excess production of outer segments, perturb intake of outer segments by the RPE secondary to physical separation of the layers, or due to RPE malfunction. Recently, results of OCT angiography studies suggested that the flow density in the superficial and deep retinal vascular layers maybe reduced in AFVD [38–40]. Querques and colleagues suggested that such vascular network modifications at the superficial and the deep capillary plexus could lead to the progression of the disease because of reduced blood supply. Another hypothesis was that the flow modification is due to a mechanical effect of the vitelliform material on blood vessels [39]. On the other hand, Toto and

colleagues found that the flow density was increased in AFVD eyes compared with AMD and normal eyes [41]. Either way, alteration of blood flow theoretically may affect the thickness of the EZ which is a highly active metabolically. Thus, our findings are in line with the presumed mechanisms that lead to the buildup of vitelliform lesions in AFVD.

Measurement of photoreceptor damage is important in monitoring the disease progression. Evaluation of the EZ band has been associated with the progression of retinal disorders such as AMD, branch retinal vein occlusion, Stargardt disease, achromatopsia, retinitis pigmentosa, and others [42]. Currently, identification and quantification of the hyper-reflective EZ band alone is not routinely used for clinical purposes and is usually done manually for research purposes. By simple manual adjustment to the automated multi-layer segmentation software, we could isolate and measured the hyper-reflective EZ layer. The accuracy of segmentation algorithms can be affected by irregularities in layer contour and/or band intensity. Indeed, segmentation errors are significantly increased in pathologic eyes when compared to normal eyes. However, by using the Bruch's membrane as a reference baseline layer we could minimize the measurement error. Automation of such a technique is an important challenge in bringing EZ quantification to the retina clinic.

This study has several limitations. The main limitation of this study is the manual adjustment of the segmented lines, which may be an operator dependent and limited in cases of disrupted normal structure of the retinal layers, however we compered between the graders and the Intraclass correlation coefficients (ICC) was high. On the other hand, the novelty of this method is that it allows EZ measuring by using the current segmentation software available on the commercial OCT machine.

Our findings support the presumed pathogenesis of AFVD. Additional research is required to identify if the primary insult in this disease lay in the photoreceptors, RPE or this physical interaction.

References

1. Chowers I, Tiosano L, Audo I, et al (2015) Adult-onset foveomacular vitelliform dystrophy: A fresh perspective. Prog Retin Eye Res 47:64–85

2. Gass JD (1974) A clinicopathologic study of a peculiar foveomacular dystrophy. Trans Am Ophthalmol Soc 72:139–156

3. Chowers I, Meir T, Lederman M, et al (2008) Sequence variants in HTRA1 and LOC387715/ARMS2 and phenotype and response to photodynamic therapy in neovascular age-related macular degeneration in populations from Israel. Mol Vis 14:2263–2271

4. Dewan A, Liu M, Hartman S, et al (2006) HTRA1 promoter polymorphism in wet age-related macular degeneration. Science 314:989–992

5. Felbor U, Schilling H, Weber BH (1997) Adult vitelliform macular dystrophy is frequently associated with mutations in the peripherin/RDS gene. Hum Mutat 10:301–309

6. Francis PJ, Schultz DW, Gregory AM, et al (2005) Genetic and phenotypic heterogeneity in pattern dystrophy. Br J Ophthalmol 89:1115–1119

7. Jaouni T, Averbukh E, Burstyn-Cohen T, et al (2012) Association of pattern dystrophy with an HTRA1 single-nucleotide polymorphism. Arch Ophthalmol 130:987–991

8. Kim RY, Dollfus H, Keen TJ, et al (1995) Autosomal dominant pattern dystrophy of the retina associated with a 4-base pair insertion at codon 140 in the peripherin/RDS gene. Arch Ophthalmol 113:451–455

9. Yang Z, Camp NJ, Sun H, et al (2006) A variant of the HTRA1 gene increases susceptibility to age-related macular degeneration. Science 314:992–993

10. Zhuk SA, Edwards AO (2006) Peripherin/RDS and VMD2 mutations in macular dystrophies with adult-onset vitelliform lesion. Mol Vis 12:811–815

11. Tiosano L, Grunin M, Hagbi-Levi S, et al (2016) Characterising the phenotype and progression of sporadic adult-onset foveomacular vitelliform dystrophy. Br J Ophthalmol 100:1476–1481

12. Arnold JJ, Sarks JP, Killingsworth MC, et al (2003) Adult vitelliform macular degeneration: a clinicopathological study. EYE 17:717–726

13. Querques G, Forte R, Querques L, et al (2011) Natural course of adult-onset foveomacular vitelliform dystrophy: a spectral-domain optical coherence tomography analysis. Am J Ophthalmol 152:304–313

14. Staurenghi G, Sadda S, Chakravarthy U, et al (2014) Proposed lexicon for anatomic landmarks in normal posterior segment spectral-domain optical coherence tomography: the IN•OCT consensus. Ophthalmology 121:1572–1578

15. Spaide RF, Curcio CA (2011) Anatomical correlates to the bands seen in the outer retina by optical coherence tomography: literature review and model: Literature review and model. Retina 31:1609–1619

16. Benhamou N, Messas-Kaplan A, Cohen Y, et al (2004) Adult-onset foveomacular vitelliform dystrophy with OCT 3. Am J Ophthalmol 138:294–296

17. Freund KB, Laud K, Lima LH, et al (2011) Acquired Vitelliform Lesions: correlation of clinical findings and multiple imaging analyses. Retina 31:13–25

18. Wakabayashi T, Fujiwara M, Sakaguchi H, et al (2010) Foveal microstructure and visual acuity in surgically closed macular holes: spectral-domain optical coherence tomographic analysis. Ophthalmology 117:1815–1824

19. Baba T, Yamamoto S, Arai M, et al (2008) Correlation of visual recovery and presence of photoreceptor inner/outer segment junction in optical coherence images after successful macular hole repair. Retina 28:453–458

20. Channa R, Ibrahim M, Sepah Y, et al (2012) Characterization of macular lesions in punctate inner choroidopathy with spectral domain optical coherence tomography. J Ophthalmic Inflamm Infect 2:113–120

21. Darugar A, Mathian A, Lehoang P, Bodaghi B (2011) Acute posterior multifocal placoid pigment epitheliopathy as the initial manifestation of sarcoidosis. J Ophthalmic Vis Res 6:338–343

22. Lee GE, Lee BW, Rao NA, Fawzi AA (2011) Spectral domain optical coherence tomography and autofluorescence in a case of acute posterior multifocal placoid pigment epitheliopathy mimicking Vogt-Koyanagi-Harada disease: case report and review of literature. Ocul Immunol Inflamm 19:42–47

23. Nguyen MHT, Witkin AJ, Reichel E, et al (2007) Microstructural abnormalities in MEWDS demonstrated by ultrahigh resolution optical coherence tomography. Retina 27:414–418

24. Yang C-S, Wang A-G, Lin Y-H, et al (2012) Optical coherence tomography in resolution of photoreceptor damage in multiple evanescent white dot syndrome. J Chin Med Assoc 75:663–666

25. Mrejen S, Sato T, Curcio CA, Spaide RF (2014) Assessing the cone photoreceptor mosaic in eyes with pseudodrusen and soft Drusen in vivo using adaptive optics imaging. Ophthalmology 121:545–551

26. Sundaram V, Wilde C, Aboshiha J, et al (2014) Retinal structure and function in achromatopsia: implications for gene therapy. Ophthalmology 121:234–245

27. Hood DC, Zhang X, Ramachandran R, et al (2011) The inner segment/outer segment border seen on optical coherence tomography is less intense in patients with diminished cone function. Invest Ophthalmol Vis Sci 52:9703–9709

28. Ha A, Kim YK, Jeoung JW, Park KH (2018) Ellipsoid zone change according to glaucoma-stage advancement. Am J Ophthalmol 192:1–9

29. Kay DB, Land ME, Cooper RF, et al (2013) Outer retinal structure in best vitelliform macular dystrophy. JAMA Ophthalmol 131:1207–1215

30. Toprak I, Yaylalı V, Yildirim C (2017) Early deterioration in ellipsoid zone in eyes with non-neovascular age-related macular degeneration. Int Ophthalmol 37:801–806

31. Tao LW, Wu Z, Guymer RH, Luu CD (2016) Ellipsoid zone on optical coherence tomography: a review: Ellipsoid zone on optical coherence tomography. Clin Experiment Ophthalmol 44:422–430

32. CK-s L, CY-l C, Rn W, et al (2008) Comparison of macular thickness measurements between time domain and spectral domain optical coherence tomography. Invest Ophthalmol Vis Sci 49:4893–4897

33. Kafieh R, Rabbani H, Kermani S (2013) A review of algorithms for segmentation of optical coherence tomography from retina. J Med Signals Sens 3:45–60

34. Lee H, Kang KE, Chung H, Kim HC (2018) Automated segmentation of lesions including subretinal hyperreflective material in neovascular age-related macular degeneration. Am J Ophthalmol 191:64–75

35. Itoh Y, Vasanji A, Ehlers JP (2016) Volumetric ellipsoid zone mapping for enhanced visualisation of outer retinal integrity with optical coherence tomography. Br J Ophthalmol 100:295–299

36. Chan A, Duker JS, Ko TH, et al (2006) Normal macular thickness measurements in healthy eyes using Stratus optical coherence tomography. Arch Ophthalmol 124:193–198

37. Chui TYP, VanNasdale DA, Elsner AE, Burns SA (2014) The association between the foveal avascular zone and retinal thickness. Invest Ophthalmol Vis Sci 55:6870–6877

38. Treder M, Lauermann JL, Alnawaiseh M, et al (2018) Quantitative changes in flow density in patients with adult-onset foveomacular vitelliform dystrophy: an OCT angiography study. Arbeitsphysiologie 256:23–28

39. Querques G, Zambrowski O, Corvi F, et al (2016) Optical coherence tomography angiography in adult-onset foveomacular vitelliform dystrophy. Br J Ophthalmol 100:1724–1730

40. Battaglia Parodi M, Rabiolo A, Cicinelli MV, et al (2018) Quantitative analysis of optical coherence tomography angiography in adult-onset foveomacular vitelliform dystrophy. Retina 38:237–244

41. Toto L, Borrelli E, Mastropasqua R, et al (2018) ADULT-ONSET FOVEOMACULAR VITELLIFORM DYSTROPHY EVALUATED BY MEANS OF OPTICAL COHERENCE TOMOGRAPHY ANGIOGRAPHY: A comparison with dry age-related macular degeneration and healthy eyes. Retina 38:731–738

42. Strampe MR, Huckenpahler AL, Higgins BP, et al (2018) Intraobserver repeatability and interobserver reproducibility of ellipsoid zone measurements in retinitis pigmentosa. Transl Vis Sci Technol 7:13

Figures
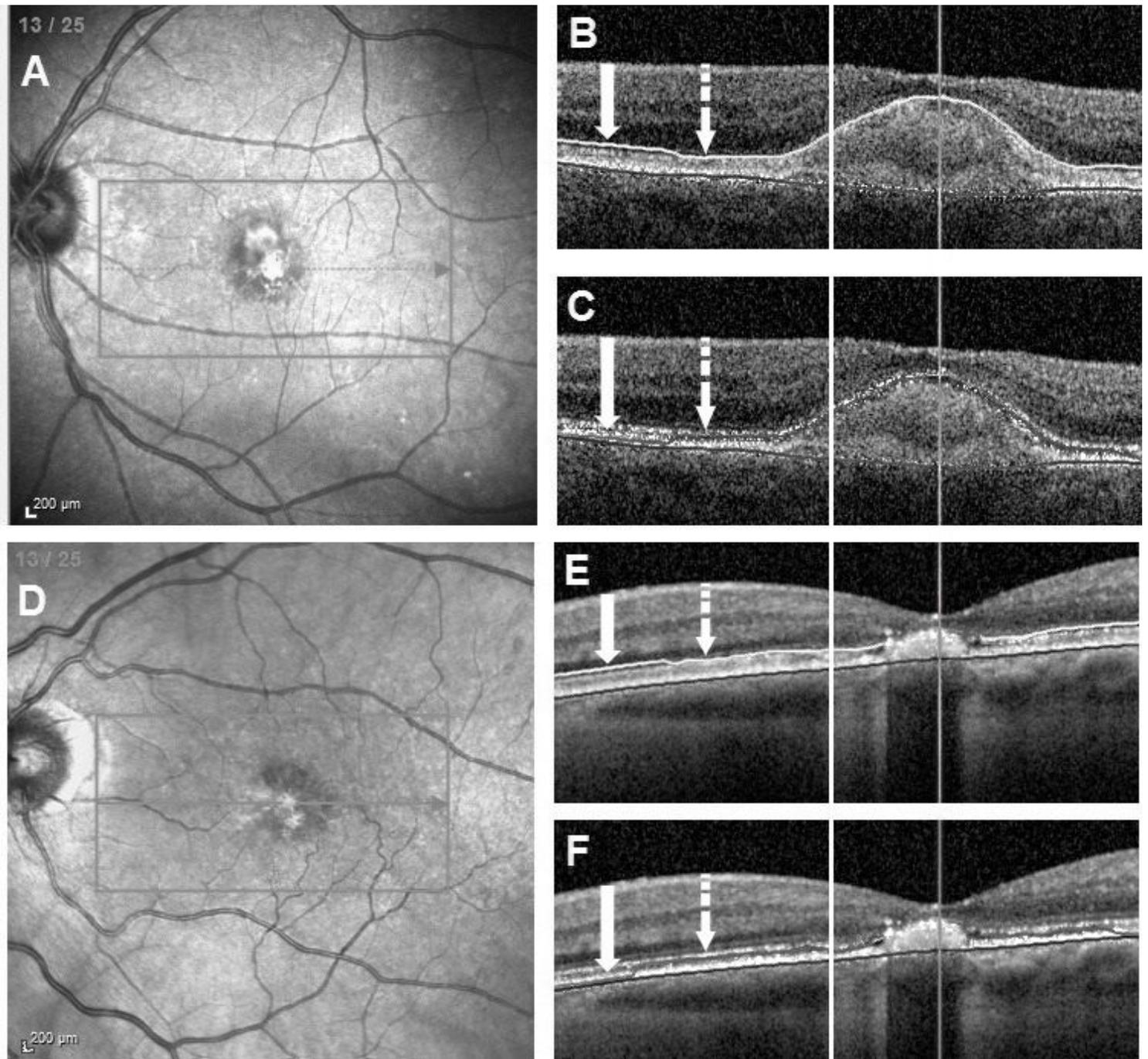
Figure 1

Measurement of Ellipsoid zone thickness – Panels A-C demonstrate the left eye of a 98-year-old female with Adult-onset foveomacular vitelliform dystrophy (AFVD) in the vitelliform stage; the visual acuity was 0.39 LogMAR. Panels D-F demonstrate the left eye of an 81-year-old male with Adult-onset foveomacular vitelliform dystrophy (AFVD) in the vitelliruptive stage; the visual acuity was 0.69 LogMAR. The white line (B, E) represents the external limiting membrane layer according to the heidelberg software segmentation (complete arrow), and the manually-corrected internal border of ellipsoid zone layer (broken arrow). In C and F the black line represents the retinal pigmented epithelium layer per the Heidelberg software (complete arrow), and the manually delineated external border of the ellipsoid zone layer (broken arrow).

We measured the ellipsoid zone thickness in fovea (grey vertical line) and at the edge of the foveal avascular zone (FAZ) 500 microns nasal to the fovea (white vertical line).
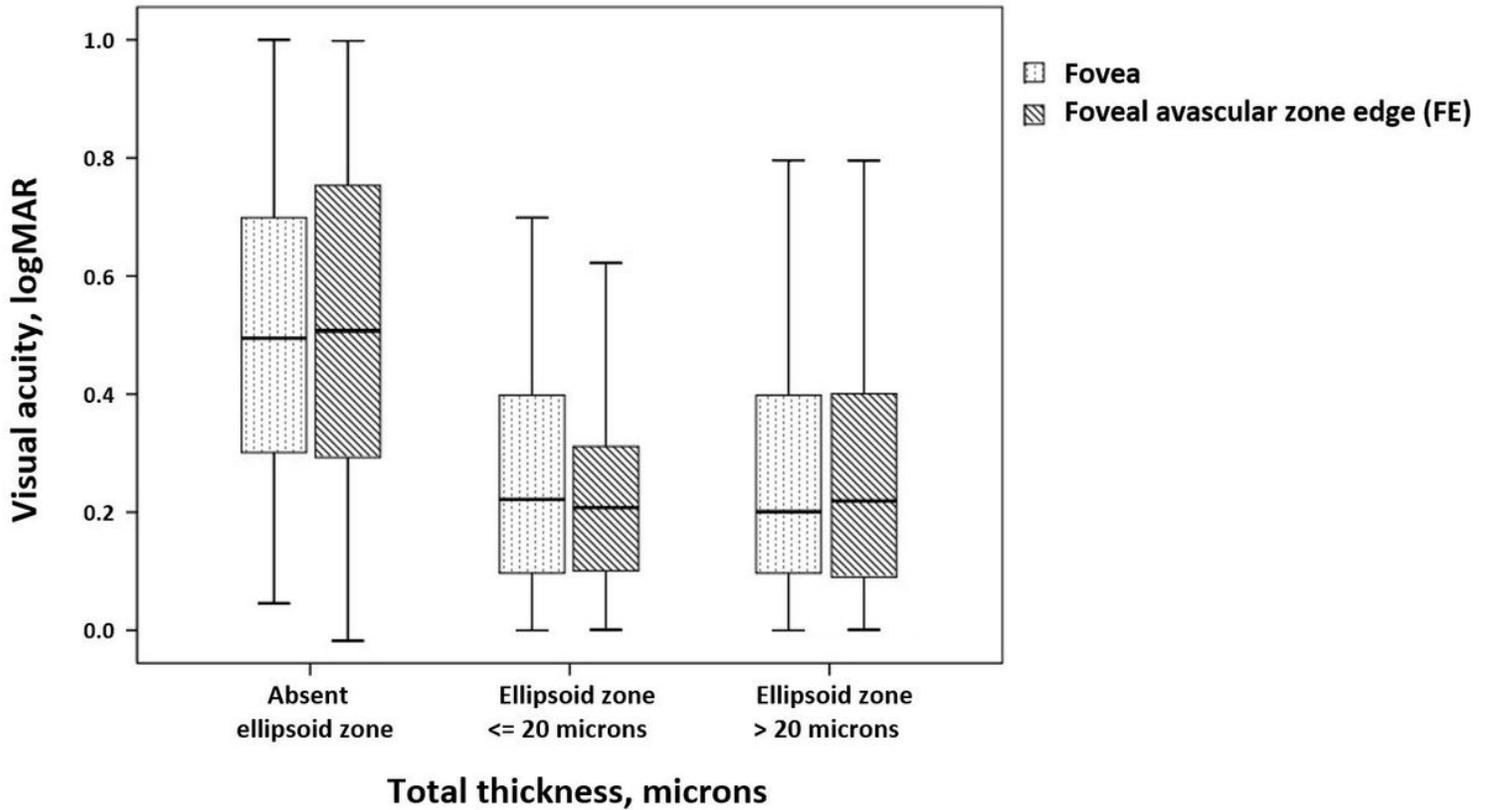

Figure 2

Association between visual acuity (LogMAR) and ellipsoid zone thickness (categorized to ≥20 micron, ≤20 micron, and no ellipsoid zone) in the center of the fovea and at the edge of the foveal avascular zone 500 microns nasal to the fovea, for the entire cohort (n=282 sections). *p<0.05 for the comparison of visual acuity between intact ellipsoid zone and absent ellipsoid zone (ANOVA test). Between the intact ellipsoid zone thickness groups (≥20, ≤20 microns) there was no significant association in the center of the fovea and at the edge of the foveal avascular zone 500 microns nasal to the fovea (p=0.28 and p=0.31, respectively, ANOVA test).